Conference Paper

Thermal characterisation of insulating layers in metal core PCB

Klarmann, S., Vagapov, Y. and Gotzig, H.

This is a paper presented at the 28th Int. Workshop on Electric Drives, Moscow, Russia, 27-29 Jan. 2021.

2021 28th International Workshop on Electric Drives: Improving Reliability of Electric Drives (IWED), Moscow, Russia. Jan 27 – 29, 2021

Thermal Characterisation of Insulating Layers in Metal Core PCB

Steffen Klarmann
Glyndwr University
Wrexham, UK

Yuriy Vagapov
Glyndwr University
Wrexham, UK

Heinrich Gotzig
Valeo S.A.
Bietigheim-Bissingen, Germany

***Abstract*—This paper provides a steady-state thermal characterisation of advanced insulating layers for isotropic electroconductive adhesive based Metal Core Printed Circuit Boards. Thermal measurements were conducted using the Thermal Transient Tester to analyse the properties of layers applied onto two different base materials – aluminium and copper. For each base material, four types of insulating layers were characterised. Size of the specimen plate for both base materials was selected as 100mm x 20mm x 1mm. The isotropic electroconductive adhesive was applied onto insulating layers to ensure electrical connection between seven SMD heat-generating components. These components are mounted in the identical distance to each other. The thermal characterisation of power SMD components and the assembling process based on isotropic electroconductive adhesive were evaluated. Application of advanced insulating layer was analysed to assess the thermal performance of complete MCPCB structure. It has been shown that the lowest thermal resistance of the aluminium based insulating layers is 21.1K/W, whereas the lowest thermal resistance of the copper based insulating layer is 15.5K/W.**

Keywords—thermal resistance, MCPCB, electroconductive adhesive, advanced insulating layer, T3Ster

I. Introduction

High power electronic semiconductors are essential components in a wide range of electrical/electronic engineering applications nowadays. The increase in the power density in such applications makes the thermal management the most crucial issue in the electronic design procedure. The high junction temperature of components affects negatively on the power semiconductor lifetime and reliability and, therefore, requires the implementation of effective methods to improve the thermal performance of cooling systems. In terms of packaging volume reduction, the electronic component thermal management systems based on printed circuit boards (PCB) properties attracted much attention in the last decades [1]. Apart from the main PCB functions to provide electrical connection between components and its housing, PCB materials are also used as a medium to transfer heat generated from high power electronic components to the ambient [2]. The thermal conductivity of various PCB materials and structures was intensively investigated using experimental and numerical approaches in the variety of studies [3]-[6]. Several manufacturing technologies have been developed and proposed to improve the thermal capabilities of PCBs. FR-4 technology is most common in the electronic industry, where PCB based heat sinks and metal filled through-holes are widely implemented to improve thermal performance [7]. The reduction in thermal resistance of PCB structure was also achieved by optimising barrel thickness of through holes and amount of copper layers within the PCB structure itself [8],[9].

In contrast to FR-4 PCBs, another, very promising PCB manufacturing technology has been discussed in recent years. This technology is based on Metal Core PCBs (MCPCB) and designed to provide improvement in the thermal properties [10]-[12]. However, it has been admitted that the most critical part of MCPCB structure is the insulating layer [13]. Many recent studies on MCPCB are focused on optimising this critical layer in terms of thermal performance improvement [14]. For example, the embedded heat pipe solutions have been proposed to decrease the junction temperature of semiconductors in high power applications [15],[16]. The thermal performance of advanced insulating layers for aluminium based MCPCB has been numerically evaluated in [17]. The experimental performance of advanced insulating layers in aluminium based MCPCBs for high power applications was demonstrated and analysed in [18]. It showed and discussed the successfully conducted process of applying high power components onto advanced insulating layers with the help of isotropic electroconductive adhesive. Consequently, MCPCB structure based on advanced insulating layers and isotropic electroconductive adhesive was successfully tested using a standard automotive grade environmental test [18].

This paper provides a steady-state thermal characterisation of advanced insulating layers for MCPCB produced using isotropic electroconductive adhesive. Thermal measurements of the layers were conducted using Thermal Transient Tester (T3Ster). Insulating layers were applied onto two different base materials – aluminium and copper. For both base material, four insulating layers were characterised. The power semiconductors used for the tests are high-power LEDs.

II. Experimental Setup

At the first step, the appropriate layer is applied onto the base material. Base material dimension selected for all specimen is 100mm x 20mm x 1mm. The actual thickness of specimen varies according to the thickness of advances insulating layers. Afterwards, the advanced insulating layers are investigated using REM/EDX (Scanning Electron Microscopy and Energy Dispersive X-ray Spectroscopy) methods. At the next step, the isotropic electroconductive adhesive is applied onto specimen with an advanced insulating layer to ensure an electrical interconnection between high-power LEDs. Finally, the thermal characterisation of the assembly is conducted using T3Ster at the steady-state condition.

A. Base Materials

Base materials selected for the test are the most common materials for MCPCB: aluminium and copper. For the aluminium base, the material Al-5052 was used.

978-0-7381-4443-6/21/$31.00 ©2021 IEEE

TABLE I. THICKNESS OF ADVANCED INSULATING LAYER.

No.	Base Material	Insulating Layer Name	Insulating Thickness (µm)
1	Al-5052	CompCoat	20
2	Al-5052	CompCoat H	30
3	Al-5052	HardCoat	30
4	Al-5052	TAL	30
5	Cu-ETP	DLC	2
6	Cu-ETP	SL1301	50
7	Cu-ETP	UHT 600	30
8	Cu-ETP	UHT Hydro	10

TABLE II. OVERVIEW EDX PARAMETERS.

	Angle (°)	Measurement Time (s)	Filtering Time (µs)	Resolution (eV)
CompCoat	28.8	30	3.84	127.6
CompCoat-H	28.8	30	3.84	127.6
HardCoat	28.8	30	3.84	127.6
TAL	28.8	30	3.84	127.6
DLC	35.2	20	0.48	132.0
SL1301	35.2	20	0.48	132.0
UHT 600	34.8	20	0.48	132.0
UHT Hydro	34.8	20	0.48	132.0

The Al-5052 thermal conductivity is $\lambda_{Al\text{-}5052}$ = 138 W/m·K. Cu-ETP was selected for the copper base material. Cu-ETP has the thermal conductivity $\lambda_{Cu\text{-}ETP}$ = 385 W/m·K.

B. Advanced Insulating Layers

A total of eight advanced insulating layers were investigated: four insulating layers are applied onto aluminium base material, whereas four insulating layers are applied onto copper base material. After this step, the specimens were encapsulated by epoxy resin to determine the microsection of each insulating layer. Finally, the thickness was determined at 6 points for each sample. Table I provides an overview of base material and appropriate insulating layers. Fig. 1 shows the microsection of aluminium samples, whereas Fig. 2 demonstrates the microsection of copper samples.

After the determination of every single layer thickness, each specimen was characterised using EDX (EDAX Apollo SDD). For all measurements, the acceleration voltage was equal to 25 kV, and the magnification was at 70. Table II shows the settings for the appropriate samples. Final results of characterisation are shown in Table III.

C. Electroconductive Adhesive

The electroconductive adhesive is applied onto every single specimen to ensure electrical interconnection between the components. Following, seven ThinGaN SMD LEDs have been applied in series connection with the identical distance between each LED. For all samples commercially available Polytec EC-242 was used as adhesive. This electroconductive adhesive is a one-component epoxy based with a silver filler. Maximum silver particle size is <30 µm, viscosity is 35,000 mPa/s, and glass transition temperature is at Tg = 110°C. Detailed electroconductive adhesive technical properties are shown in Table IV. The adhesive is applied to base material using dispensers Preeflow eco-PEN300 and Vieweg DC200. Preeflow eco-PEN300, a rotating precision-volume dispenser, has been employed using the following operating parameters: the dosing volume per revolution is 0.012 ml/rev (approx.); the pressure range is 0–6 bar; the range of volume flow is 0.12–1.48 ml/min. Dispenser Vieweg DC200 operated at the range of the flow rate between 0.5 and 6.0 ml/min and the minimum dispensing volume of 0.004 ml. The adhesive was dosed on the surface of the specimen using Vieweg TE-Series needles having a diameter of 0.33 mm. The dispenser has been attached to the robot KUKA KR30HA manipulator which operated at positioning accuracy of 0.02 mm and speed of 3 mm/s. The operating gap between the needle and the surface of the specimen was 1.8 mm. The adhesive applications were conducted at the humidity condition of 46%RH and ambient temperature of 27°C. Fig. 3a illustrates the process of isotropic electroconductive adhesive application, whereas Fig. 3b shows the installation of SMD components onto the specimen.

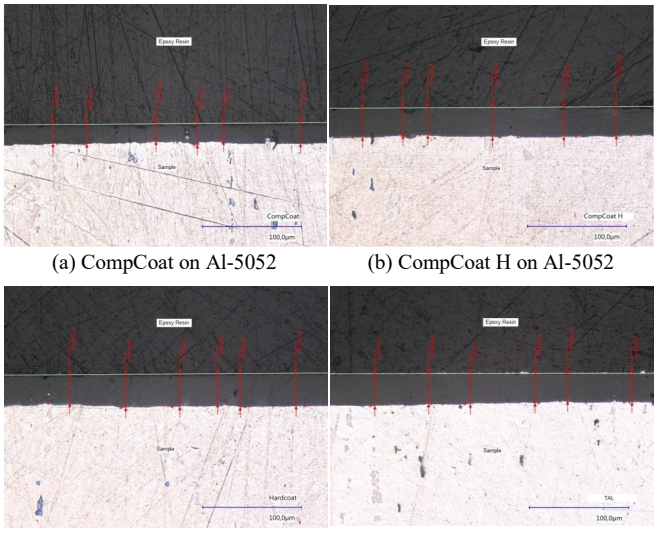

(a) CompCoat on Al-5052 (b) CompCoat H on Al-5052

(c) HardCoat on Al-5052 (d) TAL on Al-5052

Fig. 1. Microsection of advanced insulating layers on aluminium base material.

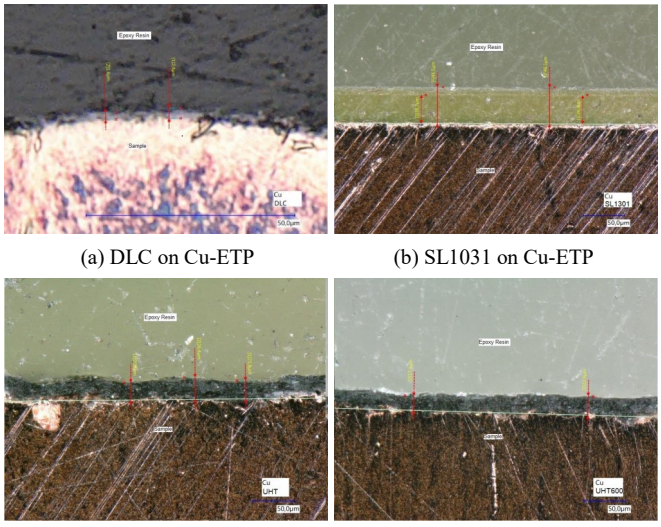

(a) DLC on Cu-ETP (b) SL1031 on Cu-ETP

(c) UHT 600 on Cu-ETP (d) UHT Hydro on Cu-ETP

Fig. 2. Microsection of advanced insulating layers on copper base material.

TABLE III. ATOMIC ELEMENT DISTRIBUTION IN ADVANCED INSULATING LAYERS BY EDX.

	CompCoat (%)	CompCoat H (%)	HardCoat (%)	TAL (%)	DLC (%)	SL1301 (%)	UHT 600 (%)	UHT Hydro (%)
Al	24.5	25.44	27.27	26.89			4.58	0.15
Ar					0.04			
C					92.41	76.6	24.92	52.17
Ca						0.14		0.10
Cl	0.06					0.01	0.11	0.09
Co						0.01		
Cr		0.02	0.02	0.02	3.04		1.46	1.75
Cu					1.51	0.11	0.77	1.21
Fe			0.03	0.02			1.09	2.96
K				0.01			1.14	0.06
Mg	1.1	1.17	0.97	0.98			0.22	1.14
Mn	0.04	0.04	0.04	0.04			0.24	1.02
Na				0.18				0.53
O	72.07	70.18	68.96	69.16		23.05	47.52	31.28
P				0.04		0.05		
S	2.2	3.06	2.46	2.42		0.03		0.04
Si	0.08	0.08	0.24	0.21	2.99		17.83	7.49
Ti							0.12	

(a) Electroconductive Adhesive (b) SMD Components

Fig. 3. Application process of MCPCB by KR30HA robot.

III. THERMAL CHARACTERISATION

A. Complete MCPCB Structure

Thermal characterisation of samples was conducted using T3Ster system. The setup of characterisation was as follows: the temperature coldplate is 25°C, the heating current is 800mA, the power step is 2.4W, the sensor current is 8mA, the heating phase is 100s, the cooling phase is 100s. The first measurement was done to determine the thermal resistance of the whole path through all layers for each LED position. Table V shows the results for aluminium samples, whereas Table VI shows the results for copper samples respectively.

TABLE IV. ADHESIVE TECHNICAL PROPERTIES.

Chemical Basis	Epoxy
Number of Components	1
Density Mix	5.3 g/cm^3
Filler Type	Silver
Maximum Particle Size	30 µm
Viscosity Mix	35,000 mPa·s
Shore D	90
Glass Transition Temperature	110°C
Specific Volume Resistivity	$5 \cdot 10^{-5}$ Ω·cm
Thermal Conductivity	4.2 W/m·K

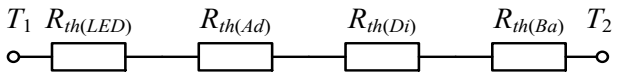

Fig. 4. Path of thermal resistance of MCPCB for T3Ster measurement.

TABLE V. THERMAL RESISTANCE OF ADVANCED INSULATING ALUMINIUM LAYERS.

LED	CompCoat (K/W)	CompCoat H (K/W)	HardCoat (K/W)	TAL (K/W)
1	30.9	24.9	19.9	25.0
2	34.3	27.17	17.0	25.9
3	27.2	27.7	16.8	23.8
4	34.4	26.2	17.6	30.9
5	34.1	31.6	33.4	27.7
6	28.8	33.9	24.0	23.5
7	40.6	42.7	19.3	29.5
Mean	32.9	28.8	21.1	26.6

TABLE VI. THERMAL RESISTANCE OF ADVANCED INSULATING COPPER LAYERS.

LED	DLC (K/W)	SL1301 (K/W)	UHT 600 (K/W)	UHT Hydro (K/W)
1	11.7	139	37.2	32.0
2	10.4	114	35.3	24.0
3	20.8	133	34.5	29.0
4	13.9	125	44.5	29.0
5	13.0	148	42.2	31.0
6	15.0	145	40.3	27.0
7	23.7	120	46.0	29.0
Mean	15.5	132	40.0	28.7

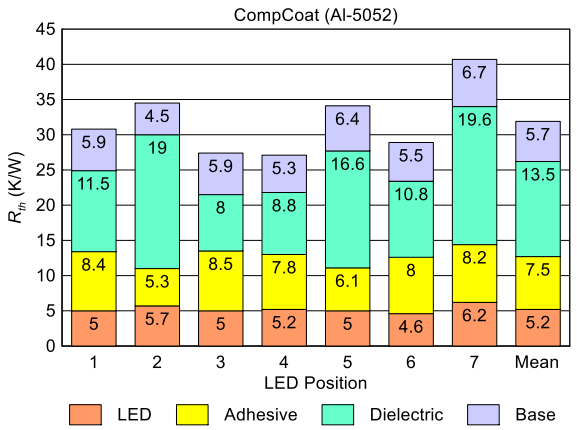

Fig. 5. T3Ster Results CompCoat on Al-5052.

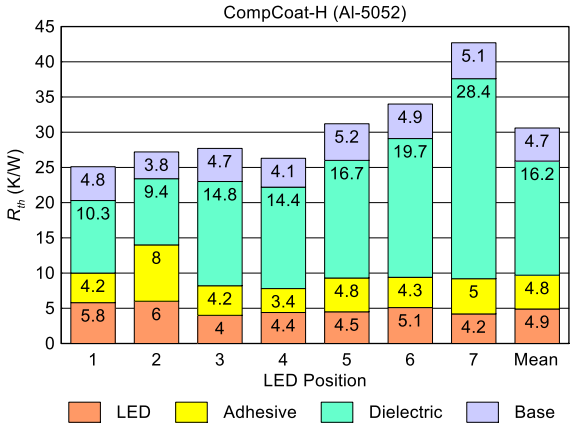

Fig. 6. T3Ster Results CompCoat-H on Al-5052.

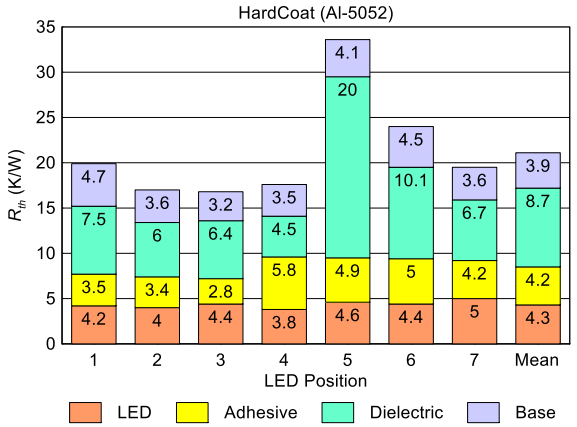

Fig. 7. T3Ster Results HardCoat on Al-5052.

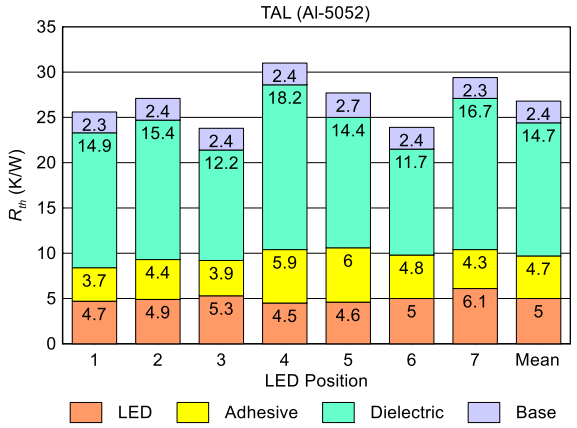

Fig. 8. T3Ster Results TAL on Al-5052.

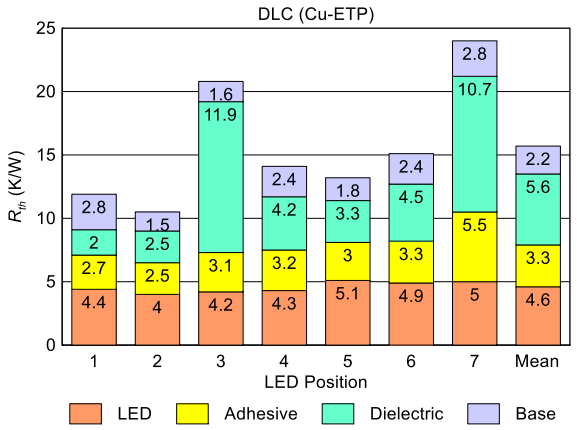

Fig. 9. T3Ster Results DLC on Cu-ETP.

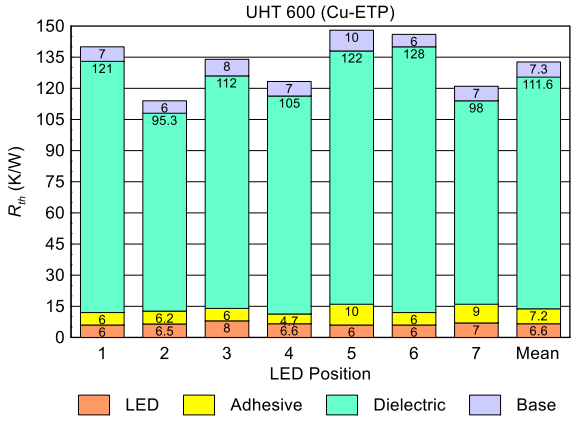

Fig. 10. T3Ster Results SL1301 on Cu-ETP.

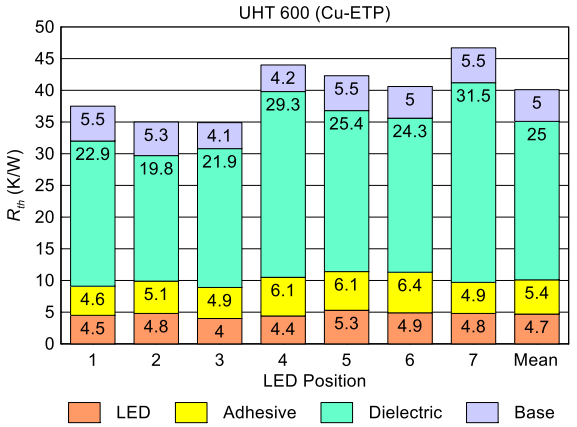

Fig. 11. T3Ster Results UHT 600 on Cu-ETP.

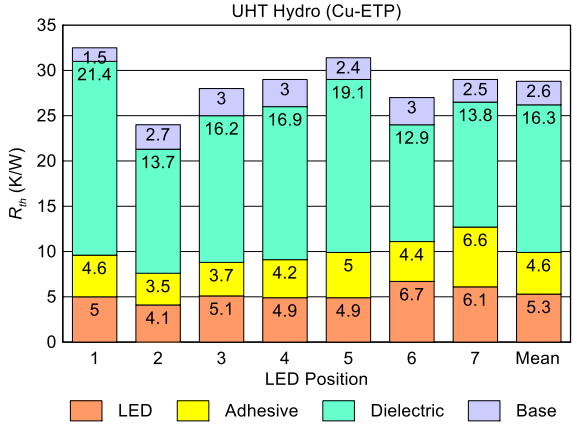

Fig. 12. T3Ster Results UHT Hydro on Cu-ETP.

B. Single Layers of MCPCB

The thermal resistance of LEDs is $R_{th} = 5$ K/W with a compensated light yield of 31%. The isotropic electroconductive adhesive is described to have a thickness of $t = 50$ µm, a contact surface $A = 1.6$ mm^2, and the thermal conductivity $\lambda = 4.2$ W/m·K. As the insulating layers vary at each specimen, the values need to be evaluated. Fig. 4 depicts the thermal resistance path for considered MCPCB in T3Ster setup, where T_1 is the ambient temperature; T_2 the temperature of the base material; $R_{th(LED)}$ is the thermal resistance of the LED; $R_{th(Ad)}$ is the thermal resistance of the isotropic electroconductive adhesive; $R_{th(Di)}$ is the thermal resistance of the advanced insulating layer; $R_{th(Ba)}$ is the thermal resistance of the base material. Figs. 5-8 show the result of T3Ster analysis for aluminium based samples, whereas Figs. 9-12 depict the results for T3Ster analysis of copper samples.

VI. Conclusion

This paper discusses the thermal property practical investigation of MCPCB insulating layers. The tests were applied for two materials: aluminium and copper, which have been used as the base for MCPCB samples. The lowest thermal resistance of four aluminium based insulating layers was achieved by HardCoat with a mean value of R_{th} = 21.1K/W. The lowest thermal resistance of the copper based insulating layer was reached by DLC with a mean value of R_{th} = 15.5K/W. However, the single-layer analysis showed that the manufacturing process of advanced insulating layers for both aluminium and copper MCPCBs has resulted in a high variance. Finally, since the thermal resistance for the electroconductive adhesive is not evenly distributed, the manufacturing process needs to be adapted to achieve homogenous results to be reproducible for future mass production of MCPCB.

References

[1] A. Kalantarian, M. Jin, J. Merkelbach, and J. Yusufali, "Evaluation of high thermal conductivity dielectric on the temperature of PCB components," in *Proc. 16th IEEE Intersociety Conf. on Thermal and Thermomechanical Phenomena in Electronic Systems*, Orlando, USA, 30 May-2 June 2017, pp. 926-929, doi: 10.1109/itherm.2017.7992585.

[2] L. Coppola, B. Agostini, R. Schmidt, and R.F. Barcelos, "Importance of boundary conditions for optimizing the thermal dimensioning of PCB traces," in *Proc. 6th Int. Conf. on Integrated Power Electronics Systems*, Nuremberg, Germany, 16-18 March 2010, pp. 1-5.

[3] J. Lohan, P. Tiilikka, P. Rodgers, C. Fager, and J. Rantala, "Experimental and numerical investigation into the influence of printed circuit board construction on component operating temperature in natural convection," *IEEE Trans. on Components and Packaging Technologies*, vol. 23, no. 3, pp. 578-586, Sept. 2000, doi: 10.1109/6144.868861.

[4] Y. Shabany, "Component size and effective thermal conductivity of printed circuit boards," in *Proc. 8th IEEE Intersociety Conf. on Thermal and Thermomechanical Phenomena in Electronic Systems*, San Diego, USA, 30 May-1 June 2002, pp. 489-494, doi: 10.1109/itherm.2002.1012496.

[5] Jin-Ju Chue, Chih-Chyau Yang, Chen-Chia Chen, Chun-Chieh Chiu, Chien-Ming Wu, and Chun-Ming Huang, "Investigation of chip temperature related to various copper thickness on glass-fabric-based substrate," in *Proc. 13th Int. Thermal, Mechanical and Multi-Physics Simulation and Experiments in Microelectronics and Microsystems*, Cascais, Portugal, 16-18 April 2012, pp. 1/6-6/6, doi: 10.1109/ESimE.2012.6191709.

[6] Y. Chen, G. Chen, and K. Smedley, "Effects of printed-circuit-board layout on power switch case-to-ambient thermal resistance," in *Proc. 29th Annual Conf. of the IEEE Industrial Electronics Society IECON'03*, Roanoke, USA, 2-6 Nov. 2003, pp. 694-698 vol.1, doi: 10.1109/IECON.2003.1280066.

[7] S. Andreev, N. Spasova, and D. Chikurtev, "Investigations on heat extraction in multilayer PCB structures," in *Proc. 27th IEEE Int. Scientific Conference Electronics*, Sozopol, Bulgaria, 13-15 Sept. 2018, pp. 1-4, doi: 10.1109/ET.2018.8549638.

[8] D.S. Gautam, F. Musavi, D. Wager, and M. Edington, "A comparison of thermal vias patterns used for thermal management in power converter," in *Proc. IEEE Energy Conversion Congress and Exposition*, Denver, USA, 15-19 Sept. 2013, pp. 2214-2218, doi: 10.1109/ECCE.2013.6646981.

[9] D. Gautam, D. Wager, F. Musavi, M. Edington, W. Eberle ,and W.G. Dunford, "A review of thermal management in power converters with thermal vias," in *Proc. 28th IEEE Annual Applied Power Electronics Conference and Exposition*, Long Beach, USA, 17-21 March 2013, pp. 627-632, doi: 10.1109/APEC.2013.6520276.

[10] H.H. Cheng, D.-S. Huang, and M.-T. Lin, "Heat dissipation design and analysis of high power LED array using the finite element method," *Microelectronics Reliability*, vol. 52, no. 5, May 2012, pp. 905-911, doi: 10.1016/j.microrel.2011.05.009.

[11] C.-P. Wang, Y.-C. Huang, and H.-Q. Liu, "Efficiency improvement of power LED modules using a hybrid aluminum nitride substrate," *Microelectronic Engineering*, vol. 223, Art. no. 111227, Feb. 2020, doi: 10.1016/j.mee.2020.111227.

[12] I. Kim, S. Cho, D. Jung, C.R. Lee, D. Kim, and B.J. Baek, "Thermal analysis of high power LEDs on the MCPCB," *Journal of Mechanical Science and Technology*, vol. 27, pp. 1493-1499, 2013, doi: 10.1007/s12206-013-0329-y

[13] S. Klarmann, B. Manesh, T. Hoenle, and Y. Vagapov, "Analysis of insulated-metal-substrates structures in the context of heat dissipation enhancement," in *Proc. 7th Int. Conf. on Internet Technologies and Applications*, Wrexham, UK, 12-15 Sept. 2017, pp. 161-164, doi: 10.1109/itecha.2017.8101929.

[14] H.M. Cho, and H.J. Kim, "Metal-core printed circuit board with alumina layer by aerosol deposition process," *IEEE Electron Device Letters*, vol. 29, no. 9, pp. 991-993, Sept. 2008, doi: 10.1109/LED.2008.2001633.

[15] W.W. Wits, and T.H.J. Vaneker, "Integrated design and manufacturing of flat miniature heat pipes using printed circuit board technology," *IEEE Trans. on Components and Packaging Technologies*, vol. 33, no. 2, pp. 398-408, June 2010, doi: 10.1109/TCAPT.2010.2041929.

[16] J.S. de Sousa, M. Unger, P. Fulmek, P. Haumer, and J. Nicolics, "Embedded mini heat pipes as thermal solution for PCBs," in *Proc. 21st European Microelectronics and Packaging Conference and Exhibition*, Warsaw, Poland, 10-13 Sept. 2017, pp. 1-6, doi: 10.23919/EMPC.2017.8346829.

[17] S. Klarmann, Y. Vagapov, and H. Gotzig, "Modelling and thermal analysis of advanced insulating layer of electronic applications," in *Proc. 24th Int. Workshop on Thermal Investigations of ICs and Systems*, Stockholm, Sweden, 26-28 Sept. 2018, pp. 1-4, doi: 10.1109/THERMINIC.2018.8593297.

[18] S. Klarmann, Y. Vagapov, and H. Gotzig, "Experimental performance analysis of advanced layers for electronic circuit boards," in *Proc. 54th Int. Universities Power Engineering Conference*, Bucharest, Romania, 3-6 Sept. 2019, pp. 1-4, doi: 10.1109/UPEC.2019.8893441.